



OPEN Ginsenoside Rg1 regulating inflammatory response and bone-remodeling through Keap1/Nrf2 signaling pathway in rats with periodontitis

Yang Zhou^{1,2,3}, Yunan Zhang^{1,2,3}, Li Wang^{1,2}, Youbo Liu^{1,2}, Zhongke Wang^{1,2} & Ling Guo^{1,2}✉

Periodontitis is a chronic inflammatory disease arising from local microorganisms and the host's own aberrant immune regulation. Ginsenoside Rg1(GS-Rg1) is an active extract of ginseng known for its anti-inflammatory and osteogenesis effects. However, GS-Rg1 has not been shown to treat periodontitis and its exact mechanism remains elucidated. Orthodontic wires inoculated with *Porphyromonas gingivalis* were wrapped around the gingiva of the first molar in rats to induce periodontitis. Inflammatory factor secretion was analyzed using RT-PCR and immunohistochemistry. The number of osteoclasts and secretion of osteogenic factors were analyzed using TRAP staining and immunofluorescence. The destruction of periodontal tissues was evaluated using Micro-CT and H&E staining. Keap1/Nrf2 pathway protein expression was analyzed using Western-Blot and RT-PCR. Applying GS-Rg1 significantly reduced the secretion of inflammatory factors IL-6 and increased the secretion of transforming growth factor TGF- β 1. Additionally, GS-Rg1 decreased osteoclast numbers and increased RUNX2 and OCN expression. Furthermore, GS-Rg1 was found to enhance the expression of the related protein Nrf2 while reducing Keap1 expression. GS-Rg1 may effectively alleviate periodontitis through the Keap1/Nrf2 pathway. In conclusion, our study provided the first preclinical evidence to support GS-Rg1 as a potential therapeutic agent for treating periodontitis.

Keywords Periodontitis, GS-Rg1, Inflammatory response, Alveolar bone remodelling, Keap1/Nrf2 signalling pathway

Abbreviations

Keap1	Kelch-like epoxychloropropane-associated protein
Nrf2	Nuclear factor erythroid-2 related factor 2
CEJ-ABC	cementoenamel junction and alveolar bone crest
BV/TV	bone volume/tissue volume

The oral cavity is a distinctive ecological niche, characterized by the presence of a diverse and specific microbial community that exists in a state of dynamic equilibrium with the host¹. However, an imbalance in the microflora, or the collective term for the microorganisms that reside in the oral cavity, can lead to an increase in periodontal pathogens and the production of many toxic substances. These toxic products can induce periodontitis by overactivating the host immune response and mediating periodontal tissue damage². One of the key microorganisms involved in this process is *Porphyromonas gingivalis*, which has the ability to disrupt host immune homeostasis³. It is a significant public health concern due to its high prevalence². Periodontitis has the potential to negatively impact chewing function and aesthetics. Furthermore, it is strongly associated with several systemic diseases, including diabetes and cardiovascular disease⁴.

¹Department of Oral Prosthodontics, The Affiliated Stomatological Hospital of Southwest Medical University, 2 Jiangyang South Road, Luzhou 646000, Sichuan, People's Republic of China. ²Oral and Maxillofacial Reconstruction and Regeneration of Luzhou Key Laboratory, The Affiliated Stomatological Hospital of Southwest Medical University, Luzhou, People's Republic of China. ³These authors contributed equally: Yang Zhou and Yunan Zhang. ✉email: glsmiling@swmu.edu.cn

Current evidence-based clinical guidelines for periodontitis recommend periodontal scaling and other physical and chemical methods of plaque removal as the mainstay of treatment⁵. Local plaque bacteria and their metabolites are the most important etiological factors and indispensable initiators of periodontal disease⁶. Antibiotics are commonly used to treat periodontitis. However, due to the rise in pathogenic bacteria resistance, the effectiveness of antibiotics is significantly limited⁷. Currently, there are now numerous small molecule drugs⁸ that focus solely on anti-inflammation⁹ or osteogenesis¹⁰. Nevertheless, only a few studies have identified both osteogenesis-promoting and anti-inflammatory agents with potential applications in periodontitis.

Ginsenoside exhibits significant pharmacological activity and holds clinical value for various applications, containing Rg, Rb, Re and other components¹¹. It has been demonstrated that specific active components of ginsenosides possess anti-inflammatory properties and exhibit excellent antibacterial and osteoclast inhibitory effects in periodontitis^{12,13}. GS-Rg1 is more abundant in ginseng roots, which also has good anti-inflammatory and antioxidant effects¹⁴. Ginsenoside Rg1 has been demonstrated to modulate periodontal membrane cellular pyroptosis and inflammatory injury, suggesting its potential as a therapeutic agent for the treatment of periodontitis¹⁵. However, in periodontitis, studies on GS-Rg1 have been limited to in vitro experiments^{15,16}. Previous research has identified the good biocompatibility of GS-Rg1 and its ability to regulate immunity by applying it to biological materials as carriers¹⁷. The modulation of immunity has been demonstrated to enhance the bone tissue microenvironment, thereby facilitating bone regeneration¹⁸. In conclusion, Rg1 can modulate immunity in rats and has been shown to have therapeutic potential for periodontitis at the cellular level.

The Keap1-Nrf2 system has been demonstrated to be integrated into a multitude of cellular signaling and metabolic pathways, thus establishing NRF2 activation as a pivotal regulatory node for a wide spectrum of disease phenotypes¹⁹. The Nrf2 factor is a crucial component of the inflammatory signaling cascade and the response to oxidative stress and is involved in a wide range of diseases, including inflammation, tumors, and neurodegenerative disorders²⁰. Recent evidence indicates that Nrf2 is crucial in protecting the host against tissue destruction in periodontitis²¹. It has been demonstrated that Nrf2 can modulate periodontitis by promoting apoptosis, inhibiting osteoclast expression, and reducing osteoblast damage²⁰. Pharmacological modulation of Nrf2 cytoprotective activity is therefore beneficial for treating periodontitis.

The objective of this study was to investigate the effect of GS-Rg1 on experimental periodontitis in rats and the specific mechanism. The hypothesis assumed in this study was that GS-Rg1 can regulate the Keap1/Nrf2 pathway to alleviate the adverse effects of periodontitis.

Results

Effects of ginsenoside Rg1 on inflammatory injury of periodontal tissue in rats with periodontitis

The chemical structure of GS-Rg1 is shown in Fig. 1A. Hematoxylin and eosin (HE) staining results showed (Fig. 1C) that the periodontal tissues in the distal-middle region of the first molar in the PD group have been destroyed, characterized by the fracture of the gingival epithelial layer, blurring of the lamina propria structure, and a notable increase in inflammatory cells within the necrotic area compared with the control group. Following the use of GS-Rg1, the mean count of inflammatory cells was decreased (Fig. 1B) and gingival epithelial integrity was restored. Furthermore, IHC staining revealed a significant increase in the mean optical density (MOD) value of IL-6 and a significant decrease in TGF- β 1 in rats in the periodontitis group. This alteration was reversed by GS-Rg1 (Fig. 1D and E), and gingival epithelial integrity was restored. Both the protein and mRNA expression of IL-6 were significantly higher in the periodontal tissues of the PD group compared to the control group, but significantly lower in the GS-Rg1 group (Fig. 1F-I), which was consistent with the results above. After using the inhibitor ML385, IL-6 expression was slightly increased, yet it remained much lower than that of the PD group (Fig. 1E and G). Conversely, TGF- β 1 protein and mRNA expression were considerably higher in the Rg1 and ML385 groups than in the PD group (Fig. 1E,I).

Effects of GS-Rg1 on alveolar bone remodeling in rats with periodontitis

Based on 3D reconstructed and cut plane images by micro-CT (Fig. 2A), the CEJ-ABC distance of PD group had grown by 2-fold compared with the control group (Fig. 2B). After the application of GS-Rg1, a reduction in the CEJ-ABC distance was observed. At the same time, the ML385 group exhibited an increase relative to the GS-Rg1 group, albeit still notably smaller than that of the PD group (Fig. 2B). This trend was consistent with the H&E staining. In addition, we quantitatively analyzed the BV/TV and BMD, which were significantly higher after Rg1 treatment compared with the PD group (Fig. 2C,D). Given that the integrity of alveolar bone hinges on the equilibrium between bone resorption and formation, the study delved into the impact of GS-Rg1 on alveolar bone regeneration in periodontitis by assessing osteoclast numbers and the expression of osteogenesis-related factors. TRAP staining showed that the PD group had more osteoclasts than the control group, and that Rg1 treatment led to a significant decrease (Fig. 2E,F). Although the employment of ML385 increased osteoclast numbers, the count remained significantly lower than that observed in the PD group. Immunofluorescence staining analysis also showed that the expression levels of RUNX2 and OCN around rats' alveolar bone after the periodontitis model were significantly lower than those of the control group. GS-Rg1 group displayed a higher RUNX2 and OCN expression intensity compared to the PD group (Fig. 3A and B). The mRNA expression of RUNX2 and OCN was significantly decreased in the PD group compared to the control group. Additionally, we noticed that mRNA levels were slightly lower in the ML385 group than in the Rg1 group, but raised in both groups when compared to the PD group (Fig. 3C). Therefore, GS-Rg1 inhibits alveolar bone loss and promotes bone formation to a certain extent in periodontitis rats, while ML385 inhibits this process.

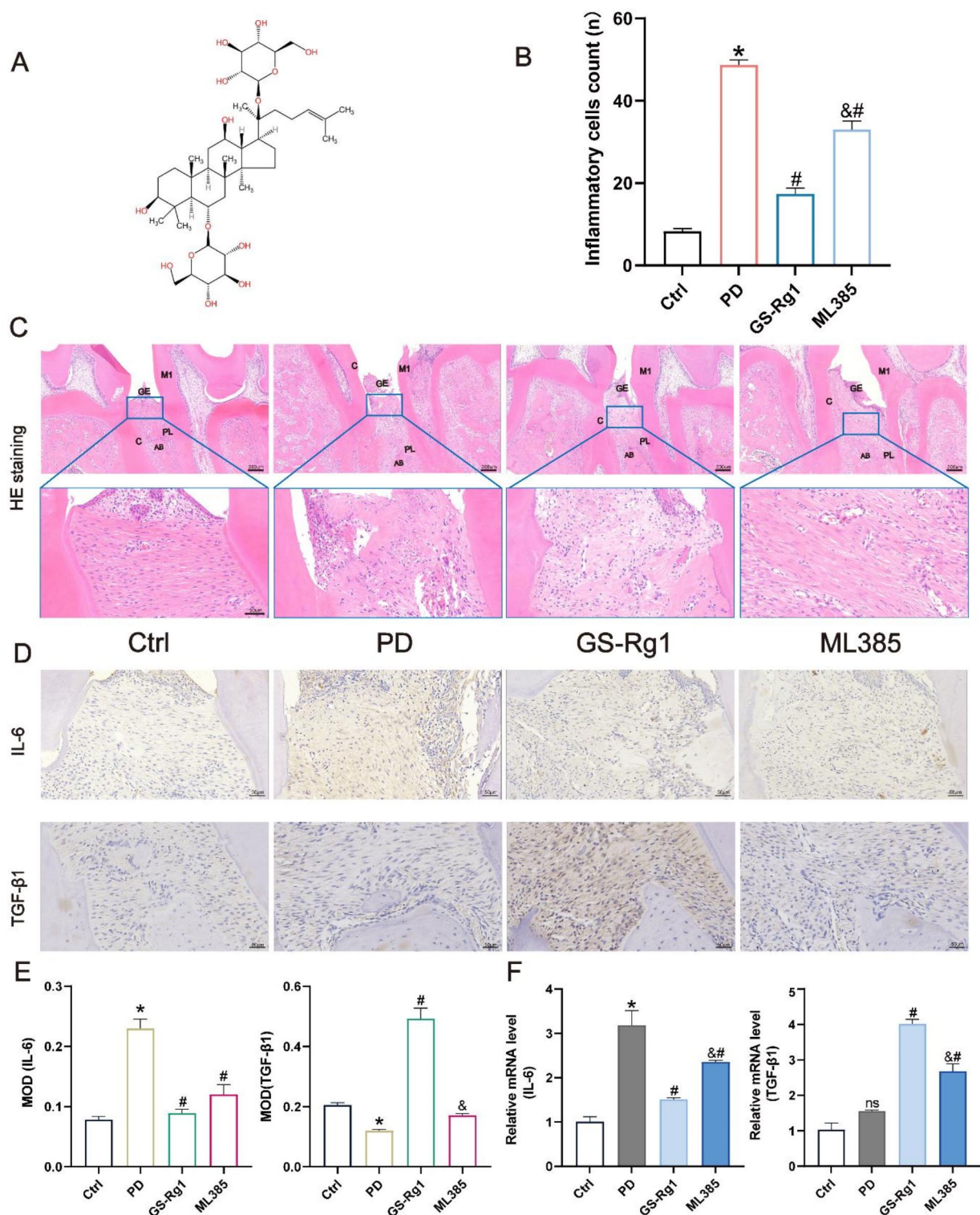


Fig. 1. Effects of GS-Rg1 on inflammatory injury of periodontal tissue. (A) Chemical structure of GS-Rg1. (B) Inflammatory cell counts of the groups(n). (C) H&E staining was used to detect the periodontal histopathological changes. M1 = first molar; C = cementum; AB = alveolar bone; GE = gingival epithelium; and PL = periodontal ligament. (D)–(F) Representative images of Immunohistochemistry (IHC) detected the expression of IL-6 and TGF- β 1 and statistical analysis of positive area. (G) and (I) qPCR quantification of the mRNA levels of IL-6 and TGF- β 1 in different groups. * $P < 0.05$, reference Ctrl; # $P < 0.05$, reference PD; & $P < 0.05$, reference GS-Rg1.

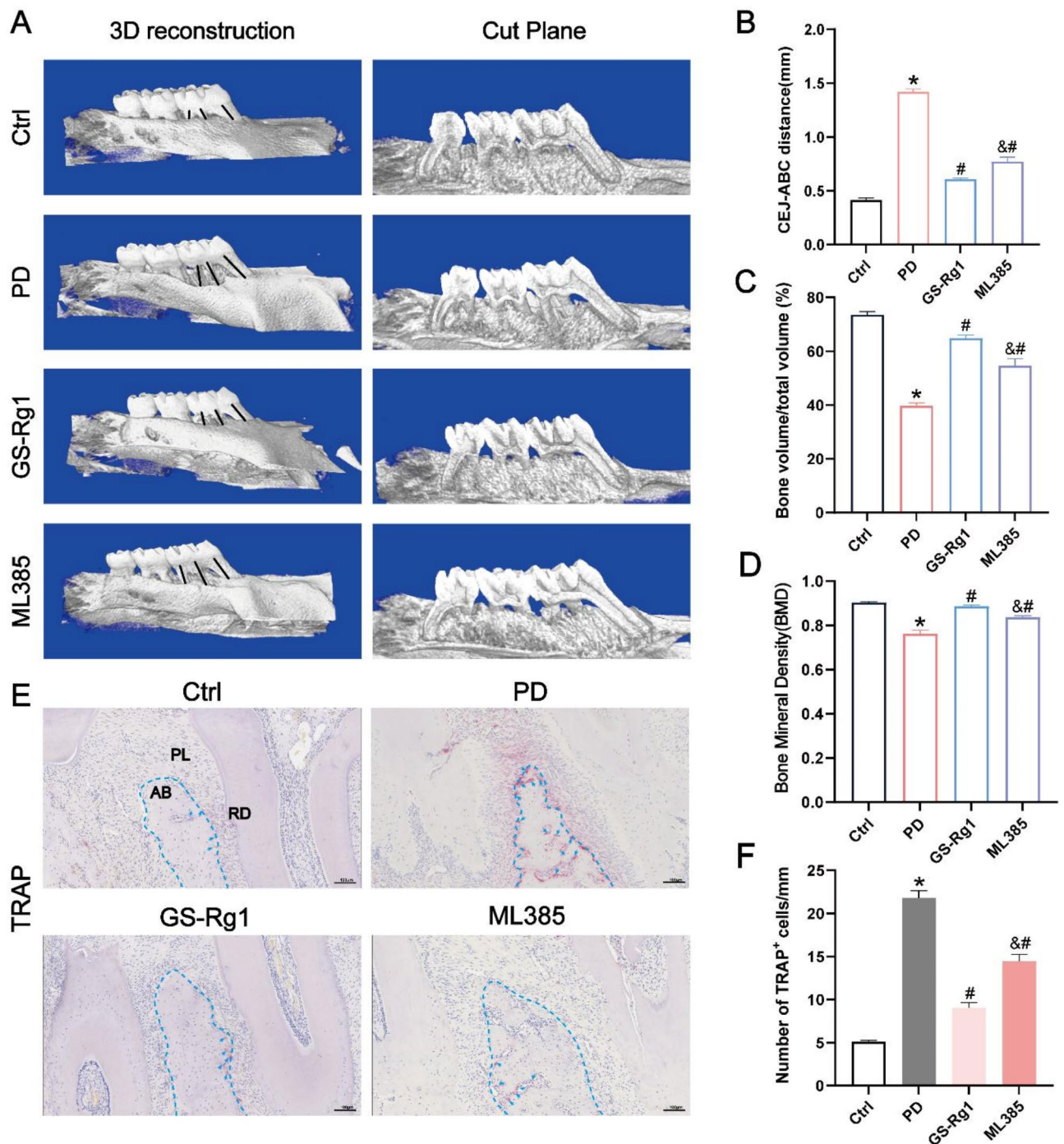


Fig. 2. Effects of GS-Rg1 on alveolar bone remodeling in rats with periodontitis. (A) Micro-CT scan imaging. (B) The linear distance (mm) from CEJ-ABC of the first molar in rats. (C) The percentage of bone volume / total volume of the standardized region of interest (ROI). (D) Bone mineral density (BMD) of the standardized region of interest (ROI). (E) Representative image of tartrate-resistant acid phosphatase (TRAP) staining. Magnification $\times 200$. The blue boxed area between 1st and 2nd molars was considered to be the region of interest for analysis of TRAP+ cells. AB = alveolar bone; PL = periodontal ligament. (F) Indicates the number of TRAP+ cells counting. * $P < 0.05$, reference Ctrl; # $P < 0.05$, reference PD; & $P < 0.05$, reference GS-Rg1.

Effects of GS-Rg1 on Keap1/Nrf2 signaling pathway in periodontitis rats

The results demonstrated that both the protein and mRNA expression of Keap1 (Figs. 3 and 4A,B) was considerably down-regulated while the protein and mRNA expression of NUC-Nrf2 was greatly enhanced when comparing the Rg1 group to the PD group. However, the use of ML385 reversed the elevated trend in the Rg1 group, and NUC-Nrf2 expression was markedly down-regulated, which was closely with that in the PD group.

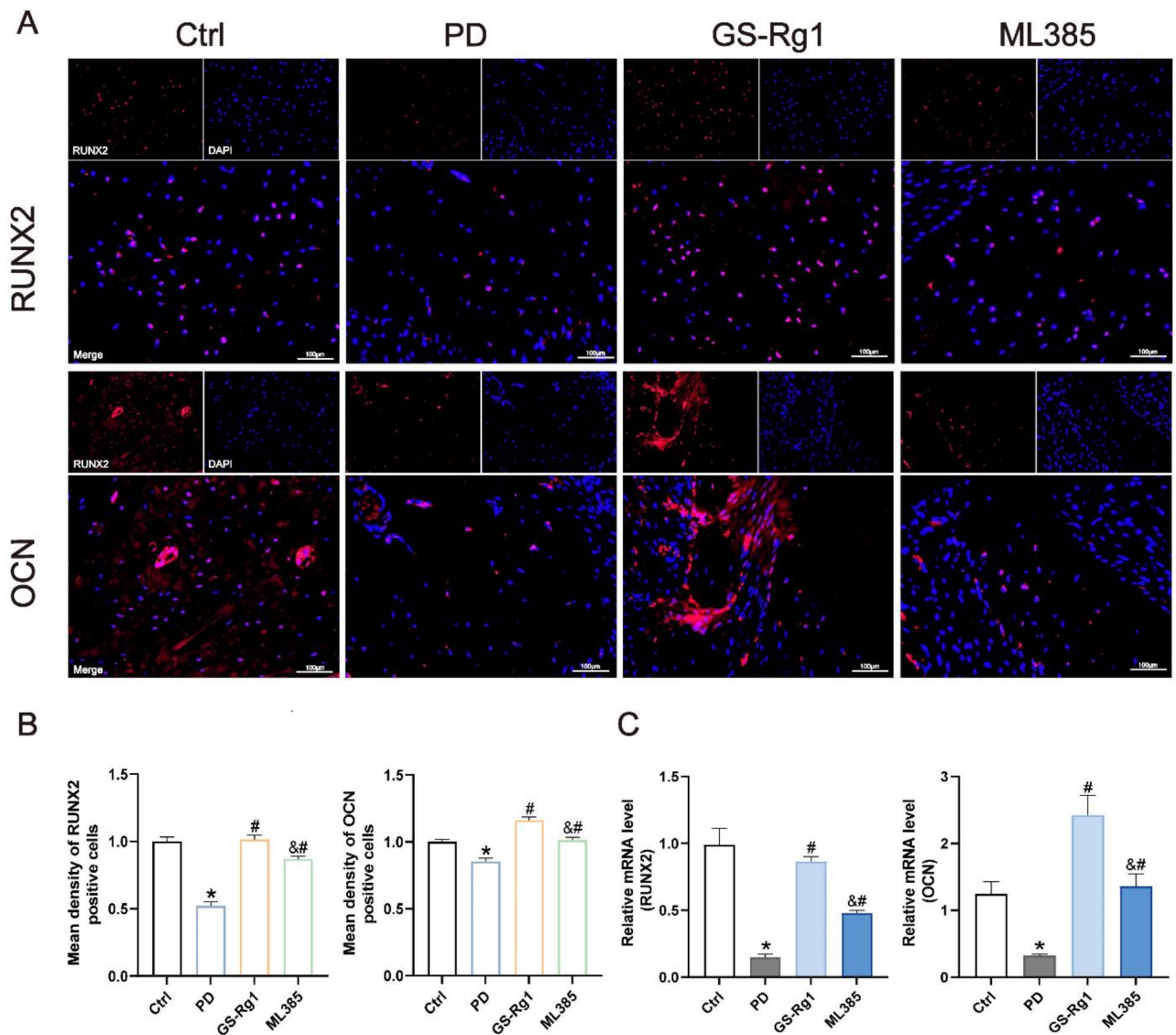


Fig. 3. Effects of GS-Rg1 on alveolar bone remodeling in rats with periodontitis. **(A)** Immunofluorescence staining of RUNX2 and OCN (red) in periodontitis tissues. **(B)** Statistical analysis of the mean staining intensity of RUNX2 and OCN. **(C)** qPCR quantification of the mRNA levels of RUNX2 and OCN in different groups. * $P < 0.05$, reference Ctrl; # $P < 0.05$, reference PD; &# $P < 0.05$, reference GS-Rg1.

(Figs. 3C and 4B, $p < 0.05$). The above results suggest that Rg1 significantly modulates the Keap1/Nrf2 signaling pathway in periodontitis rats.

Discussion

Periodontitis, the most prevalent oral disease, has a bidirectional regulatory relationship with several systemic diseases that have high mortality rates⁴. The most critical factor in the pathogenesis of periodontal disease is the enhanced interaction between microflora dysbiosis and destructive inflammation²². Pathogens affect periodontal tissue cells by modulating the immune system, thereby activating adaptive immunity as well as persistent inflammation and periodontal tissue damage²³. The ultimate consequence of periodontitis is the irreversible resorption of the alveolar bone, which ultimately results in the loosening and subsequent loss of the affected teeth²⁴. This paper investigated the regulatory effect of GS-Rg1 using rats to refine the in vivo study of Rg1 application in periodontitis. The ligation-induced periodontitis model represents an efficacious methodology for the induction of periodontitis that exhibits similarities to that observed in humans²⁵. During ligation, plaque accumulates around the ligature wire, and the placement of the ligature wire induces a continuous inflammatory infiltrate, which results in the gradual destruction of periodontal tissues²⁶. Furthermore, to align more closely with the physiological aspects of periodontitis induction, ligation wires inoculated with *Porphyromonas gingivalis* were placed around the teeth of rats to induce a significant local accumulation of periodontal pathogens²⁷.

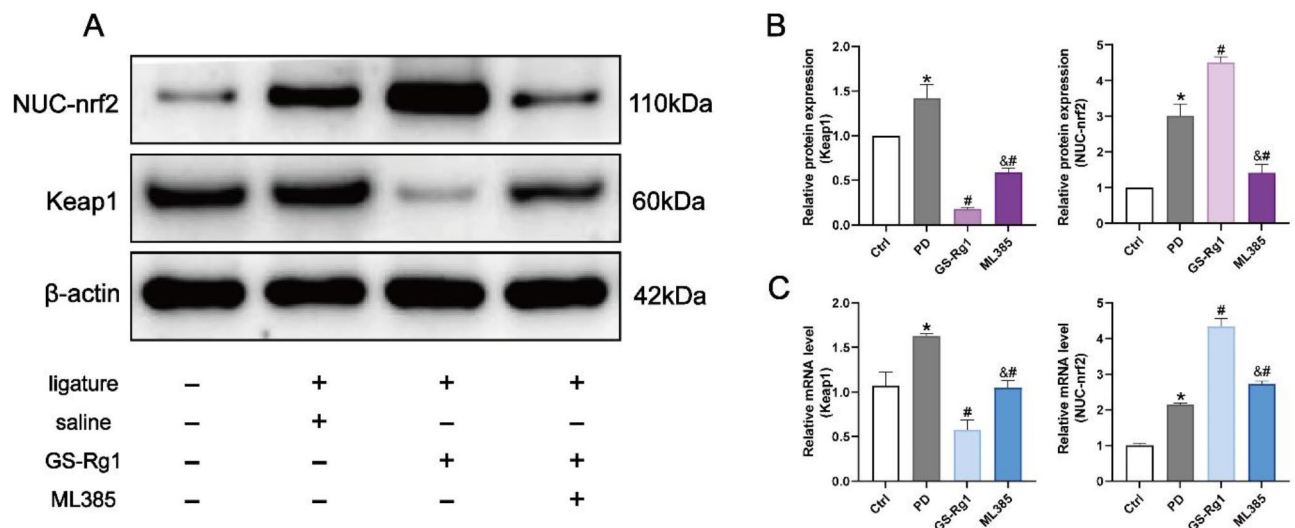


Fig. 4. Effects of GS-Rg1 on Keap1/Nrf2 signaling pathway in periodontitis rats. **(A)** The protein expressions of Keap1 and NUC-Nrf2 in periodontal tissues were detected by WB. The samples derived from the same experiment and that gels/blots were processed in parallel. The original gel imprinting is shown in the supplementary Fig. S2. **(B)** Grayscale analysis of protein bands. **(C)** qPCR quantification of the mRNA levels of Keap1 and NUC-Nrf2 in different groups. * $P < 0.05$, reference Ctrl; # $P < 0.05$, reference PD; & $P < 0.05$, reference GS-Rg1.

To the best of our knowledge, this is the first study in vivo to investigate the therapeutic mechanism of GS-Rg1 in the treatment of periodontitis. The results confirmed that GS-Rg1 effectively alleviated local periodontal inflammation and decreased alveolar bone resorption. This result is consistent with previous in vitro studies which discovered that a specific concentration of GS-Rg1 could enhance the proliferation and osteogenic differentiation of human periodontal ligament stem cells (hPDLSCs)¹⁵. A literature review has shown that ginsenosides protect target tissues from disease by acting on osteoblasts, osteoclasts, periodontal ligament fibroblasts (PDLF) and chondrocytes in bone tissue²⁸. Based on the mechanisms and previous studies, this study focused on a bioactive component extracted from ginseng. Ginseng has various therapeutic effects including antidiabetic, antitumor, antioxidant and anti-apoptotic²⁹. Most ginsenosides, representing over 80% of the total ginsenoside content, such as Rb1, Rb2, Rc, Rd, Re, Rg1, and R1, are characterized by the presence of a sugar moiety²³. This structural feature enhances the stability and solubility of these compounds, conferring a beneficial property for utilization in living organisms³⁰. Ginsenoside GS-Rg1 is the primary pharmacologically active ingredient in ginseng. It has been shown to have anti-lipid peroxidation and free radical scavenging effects, as well as promoting cell growth and regulating endothelial cell function.

The present study confirmed a greater infiltration of inflammatory cells in the gingival tissues of rats with periodontitis. These inflammatory cell locations are similar in location to the spatial sequencing results³¹. Due to unbalanced oxidative stress processes and immune dysregulation, periodontitis causes soft tissue inflammation³². Research has shown that GS-Rg1 improved tissue inflammation in diabetic rats by reducing IL-1 β and TGF- α ³³. Similarly, this study confirmed that GS-Rg1 can reduce pro-inflammatory factors like IL-6 and IL-1 β , and increase anti-inflammatory factors like TGF- β 1. The differences between rats with periodontitis and those treated with GS-Rg1 suggested that GS-Rg1 can effectively alleviate local inflammation levels by modulating inflammatory factors. One of the adverse outcomes of periodontitis is tooth loose even loss due to the destruction of periodontal tissues⁴. The analysis of Micro-CT data indicates that GS-Rg1 not only reduces bone volume resorption but also effectively mitigates changes in bone mineral density. Furthermore, osteoclast-mediated bone resorption is an important pathological process in alveolar bone resorption, which could be proved by TRAP staining. To explore the regulatory mechanisms of bone homeostasis, we confirmed a significantly decreased secretion of osteogenesis-related factors RUNX2 and OCN as well as an increase in the number of osteoclasts in periodontitis rats. The present study confirmed that GS-Rg1 application can effectively alleviate alveolar bone resorption and promote bone formation. The observed outcomes may be associated with the capacity of GS-Rg1 to modulate bone marrow mesenchymal stromal cells³⁴.

This study found that rats with periodontitis had higher expression levels of periodontal inflammation and more alveolar bone resorption. Administration of GS-Rg1 improved the aforementioned phenomena. However, co-administering it with Nrf2 inhibitors reversed the positive regulatory effect of GS-Rg1. After evaluating the effectiveness of GS-Rg1, we observed an increase in the expression of Nrf2 and a decrease in Keap1. A review has reported that Nrf2 may have a protective effect on periodontitis, although the specific effects are not yet fully understood³⁵. Nrf2 exhibits high expression and activity in monocytes, neutrophils, T cells, and B cells in the blood, indicating an immunomodulatory effect³⁶. Additionally, the study³⁷ discovered that systemic Nrf2 activation due to Keap1-deficiency, as well as T cell-specific Nrf2 activation, resulted in a decrease in IFN- γ production by effector Th1 and CTLs in the scurfy mode. The regulatory molecule Nrf2 plays a significant role

in genes expression in anti-oxidative stress and anti-inflammatory proteins²⁰. The present study demonstrated that Nrf2 inhibition increased Keap1 expression and inflammatory cell expression and related factors. Similarly, regulating the Nrf2/Keap1 pathway can reduce airway inflammation³⁸. Dysregulation of the immune system can cause inflammatory stimuli that can disrupt bone homeostasis. The present study demonstrated that the use of Nrf2 inhibitors reverses the promotion of GS-Rg1 on osteogenesis-related proteins. Restoring Nrf2 through the use of an Nrf2 agonist TBHQ (tert-butylhydroquinone) significantly reduced bone degradation and abnormal Nrf2 downstream expression of antioxidant enzymes, inflammatory cytokines, and osteogenic factors in type 2 Diabetic Osteoporosis³⁹. In this condition, Nrf2 could be activated by an endogenous pro-resolving lipid mediator to promote the osteogenic capacity of the osteoblast cell line MC3T3-E1⁴⁰. Bone metabolism is realized through bone formation and bone resorption involving osteoblasts and osteoclasts, and its metabolic activity is a dynamic equilibrium process⁴¹. The present study demonstrated that GS-Rg1 regulated the Keap1/Nrf2 pathway to reduce osteoclasts. This finding is consistent with previous study which indicated that the Keap1/Nrf2 pathway could be activated to inhibit the formation, differentiation, and bone resorption activities of osteoclasts⁴². Above all, we can speculate that the beneficial effect of Nrf2 against periodontitis can be achieved through the modulation of inflammatory factors, balancing osteogenic and osteoclast activity, and regulating the proliferation and apoptosis of periodontally-related cells. Therefore, we can conclude that ginsenoside GS-Rg1 positively affects the treatment of periodontitis through the Keap1/Nrf2 signaling pathway.

In vitro studies to verify the mechanism of action of GS-Rg1 in periodontitis could not be performed in this study. Experimental animal periodontitis can to some extent recapitulate the clinical, molecular, and histological features of human periodontitis, which is more credible in probing drug action⁴³. However, the deeper mechanisms of Rg1-regulated periodontitis should be explored at the cellular level. Therefore, it is necessary to further determine the mechanism of action of Rg1 in periodontal tissue-associated cells.

Conclusion

A classical rat periodontitis model was established in this study. It was confirmed that GS-Rg1 could effectively alleviate periodontal inflammation, reduce the number of osteoclasts, increase osteogenic activity, alleviate pathological damage to periodontal tissues, and prevent tooth loosening caused by alveolar bone resorption. The inhibition of the Keap1/Nrf2 pathway was found to reverse these effects. This study confirms that GS-Rg1 can regulate the Keap1/Nrf2 pathway to alleviate the adverse effects of periodontitis. The findings provide scientific data for the translational clinical application of GS-Rg1 and suggest a new direction for the treatment protocol of periodontitis.

Methods

Animals

The experimental protocol was approved by the Laboratory Animal Ethics Committee of Southwest Medical University (Approval NO.:2023030). The entire experiment followed the ARRIVE guidelines and the American Veterinary Medical Association (AVMA) Guidelines for the Euthanasia of Animals (2020). Thirty-two 8-week-old male SD rats (220 ± 10 g) were purchased from the Laboratory Animal Center of Southwest Medical University. The rats received a standard chow diet and were housed in separate cages with controlled temperature settings of 22–25 °C, 50–65% humidity and a 12-h light/dark cycle, six per cage. The study was also carried out complied with the ARRIVE guidelines and all protocols were in compliance with the Guide for the Care and Use of Laboratory Animals published by the NIH.

Experimental design

The rats were randomly (Random Number Generators) divided into four groups ($n=8$ /group, according to PASS 2023(S1) based on the data of previous results), including Ctrl group (no ligature + saline), PD group (ligature + saline), Rg1 group (ligature + 1 mg/ml Rg1), ML385 group (ligature + 1 mg/ml Rg1 + 1 mg/ml ML385, an inhibitor of Nrf2). The sample size was determined using power analysis with PASS software. (1) The optimal sample size needed to achieve 80% power in the statistical analysis of the data was calculated based on pre-experiment, and a 95% confidence interval. (2) The minimum number of animals required was two per experimental group. To ensure that each experiment could be replicated in three samples, we chose eight rats per group. Based on previous studies¹³ combined with our pre-experiments on modeling periodontitis in rats (S2), it was shown that periodontitis can be observed in 3 weeks of modeling. The rats were placed in an airtight container and injected with 4% (v/v) isoflurane until completely anesthetized, then a 0.20 mm diameter orthodontic wire ring was lapped at the neck of the upper first molar for 3 weeks (Fig. 5A). Check the ligature to ensure it is firmly in place and apply *Porphyromonas gingivalis* suspension to the ligature wire daily.

At the end of three weeks, the ligature wire around the first molar of the rat was removed. The Rg1 group was injected daily for two weeks with 3ul Rg1 (1 mg/ml in saline, 22427-39-0, Weiweiqi Biotech, China) into the gingival sulcus around the first molar using a microsyringe. Subsequently, the ML385 group received local injections of the inhibitor ML385 (1 mg/ml in saline, HY-100523, MedChemExpress, China) thirty minutes post-Rg1 injection. Meanwhile, the PD and Ctrl group received the same volume of saline as previously described. Each rat's operation was performed in the same order and returned to its original cage when completed. On day 35, rats were given prolonged inhalation of isoflurane for respiratory depression for the purpose of euthanasia and samples were collected for later experiments (Fig. 5B).

Micro-computed tomography (Micro-CT)

The bilateral maxillae of rats were fixed in 4% paraformaldehyde and scanned using Sky Scan 1176 desktop X-ray micro-CT system (Bruker, USA). In this study, the X-ray source was set at 65 kV, 385μA and 18 μm resolution.

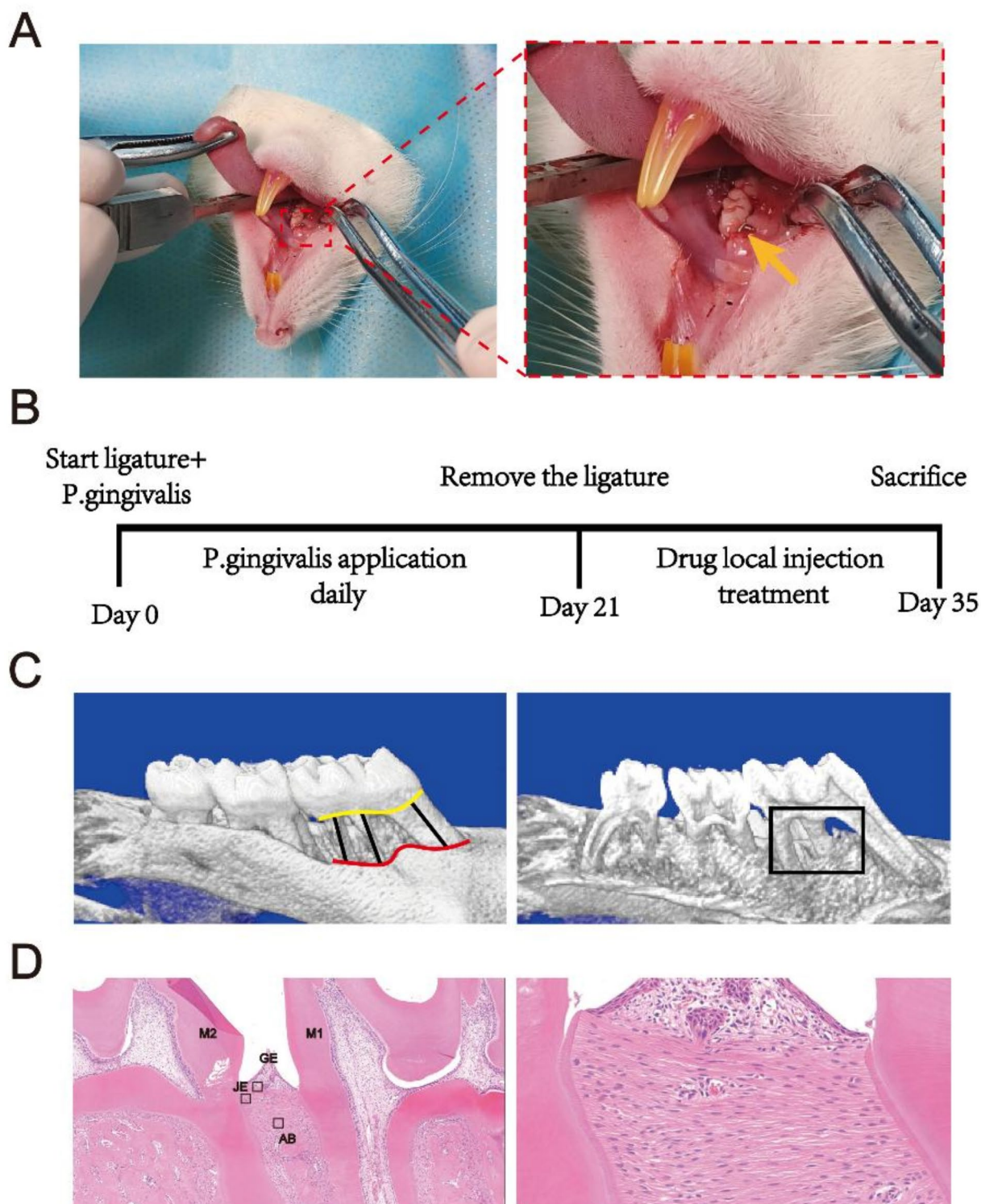


Fig. 5. Experimental model and analysis area diagram of periodontitis in rats. **(A)** Construction of rat periodontitis model **(B)** Protocol and time flow chart of this study **(C)** Yellow line represents cemento enamel junction (CEJ), red line represents crest of the alveolar bone (ABC), and the black box indicates the selection of an ROI to calculate the distance from CEJ to ABC, BV/TV (%) and BMD in the 3D reconstructed image. **(D)** Representative histological images, with three consecutive square views from the conjunctive epithelium (JE) to the gingival epithelium (GE) and alveolar bone (AB) showing the target area for counting inflammatory cells in the periodontal tissue of rats.

Gene	Primer sequence
IL-1 β -F	GGGATGATGACGACCTGCT
IL-1 β -R	CCACTTGTGGCTTATGTTCTG
IL-6-F	AAATCTGCTCTGGTCTTCTGG
IL-6-R	ACTCTGGCTTTGTCTTCTTG
TGF- β 1-F	ACCGCAACAACGCAATCTAT
TGF- β 1-R	ACCAAGGTAACGCCAGGAAT
RUNX2-F	GGACGAGGCAAGAGTTTCAC
RUNX2-R	ACTGGGATGAGGAATGCG
OCN-F	GGAGGGCAGTAAGGTGGTGAA
OCN-R	GAAGCCAATGTGGTCCGCTA
TLR4-F	ATGAGGACTGGGTGAGAAACG
TLR4-R	ACCAACGGCTCTGGATAAAG
GAPDH-F	CAAGTTCACGGCACAG
GAPDH-R	CCAGTAGACTCCACGACAT

Table 1. Primers sequences for the analysis of target genes by RT-PCR.

Finally, CTvox (Bruker, USA) software was used for 3D reconstruction. Selection of an area at the first molar as a region of interest (ROI) for analysing the linear distance from the dentin-enamel junction (CEJ) to the alveolar bone crest (ABC, mm), the bone volume fraction (BV/TV, %) and bone mineral density (BMD, g/cm²) was shown in Fig. 5C.

Hematoxylin & Eosin (H&E) staining and quantification of osteoclasts

The maxillae were collected and fixed for 24 h in 4% paraformaldehyde solution and then decalcified for 4 weeks at 10 °C in 8% EDTA solution. The decalcified specimens were dehydrated, embedded in paraffin, and sectioned at a thickness of 5.0 μ m for hematoxylin and eosin (H&E) staining. The interest area analysed for inflammatory cells in periodontal tissue was shown in Fig. 5D⁴⁴.

A part of each tissue section was stained with the TRAP staining kit (G1050, Servicebio, China) following the manufacturer's instructions, and counter-stain with hematoxylin. Red multinucleated cells, defined as active osteoclasts, were observed to form three or more nuclei on the apical and peripheral surfaces of the alveolar bone around the first molar.

Immunohistochemistry (IHC) analysis

Tissue sections were subjected to IHC staining to detect the levels of IL-6 and TGF- β 1 using an IHC accessory kit. Then the anti-IL-6 antibody (GB11117, 1:200, Servicebio, China) and anti-TGF- β 1 antibody (GB11179, 1:500, Servicebio, China) were prepared in the sections following the protocol provided. The secondary antibody (GB23303, 1:200, Servicebio, China) conjugated to peroxidase was then added, and left for 50 min at room temperature. Antibody binding was detected with a diaminobenzidine solution (G1212, 1:1000, Servicebio, China). Next, the slides were counterstained with hematoxylin. Finally, stained slides were examined with a microscope (E100, Nikon, Japan). Staining with brown-yellow was regarded as positive signal. Five areas of periodontal tissue between the gingival epithelium and the tip of the alveolar bone in the distal middle of the first molar were randomly selected and mean optical density (MOD) values were measured using Image J FIJI image analysis system.

Immunofluorescence staining

Paraffin sections were sealed with 5% BSA after deparaffinization and antigen retrieval. After blocking, the slices were incubated overnight at 4 °C with primary antibodies against OCN (16157-1-AP, 1:200, proteintech, USA) and Runx2 (20700-1-ap, 1:200, proteintech, USA). After three rinses with phosphate buffer solution, the slices were then treated with Alexa Fluor 488-labelled secondary antibodies (GB23303, 1:200, Servicebio, China). The nuclei were counter-stained for 10 min with 4',6-diamidino-2-phenylindole 147 (DAPI, 2 μ g/ml, G1012, Servicebio, China) and mounted with anti-fade prolong reagent (G1401, Servicebio, China). Images were captured with a fluorescence microscope (IX73, OLYMPUS, Japan). For the immunofluorescence analysis, the apical end of the alveolar ridge in and around the distal middle of the first molar in rats was targeted, and five areas were randomly selected for quantitative analysis.

Quantitative real-time polymerase chain reaction (qPCR)

The gingiva was removed from the first molar of the maxilla and stored at -80 °C. Total RNA was extracted from gingival tissues by Trizol (15596026, Ambion, USA) and reverse transcription. The prepared cDNA was amplified by PCR. The expression levels were calculated by using the $2^{-\Delta\Delta CT}$ method normalized to that of GAPDH. Table 1 shows the sequences for the relevant primers used in this test.

Western blotting (WB)

The sample tissue was cut into tiny pieces and lysate was added at a ratio of 200 μ L of lysate per 20 mg of tissue to extract proteins. Protein extracts were separated by PAGE glue and then transferred to PVDF membranes (IPVH00010, Millipore, USA). After blocking with 5% skimmed milk at 4 °C overnight, incubated membranes at room temperature for 1 h with primary antibodies recognizing Keap1, Nrf2 and β -actin proteins (1:1000, all from Bioswamp, China). After blocking with 5% skimmed milk at 4 °C overnight, incubated membranes at room temperature for 1 h with primary antibodies recognizing Keap1, Nrf2 and β -actin proteins (1:1000, all from Bioswamp, China). Following three rinses with phosphate buffer solution, which took 5 min each, the membranes were then incubated for 1 h at room temperature with the second antibody (1:10000, SAB48169, Bioswamp, China). The protein bands were scanned by an Odyssey[®] CLx Infrared Imaging System and quantified by ImageJ software (National Institutes of Health).

Statistical analysis

All experiments were performed in triplicate and repeated at least three times. GraphPad Prism 9.5 software (GraphPad Software, Inc., La Jolla, CA, USA) was applied for statistical analysis. All data were found to be normally distributed and were shown as mean \pm standard error of the mean (SEM). Statistical comparisons were performed using one-way analysis of variance (ANOVA) and post hoc test (Tukey test) for differences among multiple groups. $p < 0.05$ was considered statistically significant. * $P < 0.05$, reference Ctrl; # $P < 0.05$, reference PD; & $P < 0.05$, reference GS-Rg1.

Data availability

Data is provided within the manuscript or supplementary information files.

Received: 30 October 2024; Accepted: 25 February 2025

Published online: 03 March 2025

References

- Peng, X. et al. Oral microbiota in human systematic diseases. *Int. J. Oral Sci.* **14**. <https://doi.org/10.1038/s41368-022-00163-7> (2022).
- Slots, J. Periodontitis: facts, fallacies and the future. *Periodontol* **2000**, *75*, 7–23. <https://doi.org/10.1111/prd.12221> (2017).
- Jia, L. et al. Pathogenesis of important virulence factors of Porphyromonas gingivalis via Toll-Like receptors. *Front. Cell. Infect. Microbiol.* **9**, 262. <https://doi.org/10.3389/fcimb.2019.00262> (2019).
- Khumaedi, A. I., Purnamasari, D., Wijaya, I. P. & Soeroso, Y. The relationship of diabetes, periodontitis and cardiovascular disease. *Diabetes Metab. Syndr.* **13**, 1675–1678. <https://doi.org/10.1016/j.dsx.2019.03.023> (2019).
- Sanz, M. et al. Treatment of stage I–III periodontitis—The EFP S3 level clinical practice guideline. *J. Clin. Periodontol.* **47**, 4–60. <https://doi.org/10.1111/jcpe.13290> (2020).
- Herrera, D., Alonso, B., León, R., Roldán, S. & Sanz, M. Antimicrobial therapy in periodontitis: the use of systemic antimicrobials against the subgingival biofilm. *J. Clin. Periodontol.* **35**, 45–66. <https://doi.org/10.1111/j.1600-051X.2008.01260.x> (2008).
- Teughels, W. et al. Adjunctive effect of systemic antimicrobials in periodontitis therapy: A systematic review and meta-analysis. *J. Clin. Periodontol.* **47** Suppl 22, 257–281. <https://doi.org/10.1111/jcpe.13264> (2020).
- Chatzopoulos, G. S., Koidou, V. P. & Tsalikis, L. Local drug delivery in the treatment of furcation defects in periodontitis: a systematic review. *Clin. Oral Investig.* **27**, 955–970. <https://doi.org/10.1007/s00784-023-04871-0> (2023).
- Sun, Y. et al. A versatile nanocomposite based on nanoceria for antibacterial enhancement and protection from aPDT-aggravated inflammation via modulation of macrophage polarization. *Biomaterials* **268**, 120614. <https://doi.org/10.1016/j.biomaterials.2020.120614> (2021).
- Zhou, C. C. et al. Osteogenesis, Osteoclastogenesis and their Crosstalk in Lipopolysaccharide-induced Periodontitis in Mice. *Chin. J. Dent. Res.* **24**, 33–39. <https://doi.org/10.3290/j.cjdr.b1105871> (2021).
- Li, Z. Y. et al. Network pharmacology analysis and animal experiment validation of neuroinflammation inhibition by total ginsenoside in treating CSM. *Phytomedicine* **126**, 155073. <https://doi.org/10.1016/j.phymed.155073> (2024).
- Lee, W. J. et al. Ameliorative effect of ginsenoside Rg6 in periodontal tissue inflammation and recovering damaged alveolar bone. *Molecules* **29** (46). <https://doi.org/10.3390/molecules29010046> (2023).
- Zhou, S. et al. Application of ginsenoside Rd in periodontitis with inhibitory effects on pathogenicity, inflammation, and bone resorption. *Front. Cell. Infect. Microbiol.* **12**, 813953. <https://doi.org/10.3389/fcimb.2022.813953> (2022).
- Yang, S. J. et al. Ginsenoside Rg1 in neurological diseases: From bench to bedside. *Acta Pharmacol. Sin.* **44**, 913–930. <https://doi.org/10.1038/s41401-022-01022-1> (2023).
- Chu, K. et al. Ginsenoside Rg1 alleviates lipopolysaccharide-induced pyroptosis in human periodontal ligament cells via inhibiting Drp1-mediated mitochondrial fission. *Arch. Oral Biol.* **147**, 105632. <https://doi.org/10.1016/j.archoralbio.2023.105632> (2023).
- Yin, L. et al. Effects of ginsenoside Rg-1 on the proliferation and osteogenic differentiation of human periodontal ligament stem cells. *Chin. J. Integr. Med.* **21**, 676–681. <https://doi.org/10.1007/s11655-014-1856-9> (2015).
- Xu, J. et al. In situ photo-crosslinked hydrogel promotes oral mucosal wound healing through sustained delivery of ginsenoside Rg1. *Front. Bioeng. Biotechnol.* **11**, 1252574. <https://doi.org/10.3389/fbioe.2023.1252574> (2023).
- Long, J. et al. Regulation of osteoimmune microenvironment and osteogenesis by 3D-Printed PLAG/black phosphorus scaffolds for bone regeneration. *Adv. Sci. (Weinh.)* **10** (2302539). <https://doi.org/10.1002/adv.202302539> (2023).
- Baird, L. & Yamamoto, M. The molecular mechanisms regulating the KEAP1-NRF2 pathway. *Mol. Cell. Biol.* **40** (e00099–20). <https://doi.org/10.1128/MCB.00099-20> (2020).
- Ma, F. et al. The role of Nrf2 in periodontal disease by regulating lipid peroxidation, inflammation and apoptosis. *Front. Endocrinol. (Lausanne)* **13**, 963451. <https://doi.org/10.3389/fendo.2022.963451> (2022).
- Chiu, A. V., Saigh, M. A., McCulloch, C. A. & Glogauer, M. The Role of Nrf2 in the Regulation of Periodontal Health and Disease. *J. Dent. Res.* **96**, 975–983. <https://doi.org/10.1177/0022034517115007> (2017).
- Hajishengallis, G. et al. Complement-Dependent mechanisms and interventions in periodontal disease. *Front. Immunol.* **10**, 406. <https://doi.org/10.3389/fimmu.2019.00406> (2019).
- Sima, C., Viniegra, A. & Glogauer, M. Macrophage Immunomodulation in chronic osteolytic diseases—the case of periodontitis. *J. Leukoc. Biol.* **105**, 473–487. <https://doi.org/10.1002/JLB.1RU0818-310R> (2019).
- Kwon, T., Lamster, I. B. & Levin, L. Current Concepts in the Management of Periodontitis. *Int. Dent. J.* **71**, 462–476. <https://doi.org/10.1111/idj.12630> (2021).

25. de Molon, R. S. et al. Long-term evaluation of oral gavage with periodontopathogens or ligature induction of experimental periodontal disease in mice. *Clin. Oral Investig.* **20**, 1203–1216. <https://doi.org/10.1007/s00784-015-1607-0> (2016).
26. Cui, Y. et al. Melatonin Engineering M2 Macrophage-Derived Exosomes Mediate Endoplasmic Reticulum Stress and Immune Reprogramming for Periodontitis Therapy. *Adv Sci (Weinh)* **10**, e2302029. <https://doi.org/10.1002/adv.202302029> (2023).
27. Lin, P. et al. Application of Ligature-Induced Periodontitis in Mice to Explore the Molecular Mechanism of Periodontal Disease. *Int. J. Mol. Sci.* **22**, 8900. <https://doi.org/10.3390/ijms22168900> (2021).
28. Ko, S. Y. Therapeutic Potential of Ginsenosides on Bone Metabolism: A Review of Osteoporosis, Periodontal Disease and Osteoarthritis. *Int. J. Mol. Sci.* **25**, 5828. <https://doi.org/10.3390/ijms25115828> (2024).
29. Qin, Q. et al. Ginsenoside Rg1 ameliorates cardiac oxidative stress and inflammation in streptozotocin-induced diabetic rats. *Diabetes Metab. Syndr. Obes.* **12**, 1091–1103. <https://doi.org/10.2147/DMSO.S208989> (2019).
30. Chopra, P. et al. Phytochemistry of ginsenosides: recent advancements and emerging roles. *Crit. Rev. Food Sci. Nutr.* **63**, 613–640. <https://doi.org/10.1080/10408398.2021.1952159> (2023).
31. Shen, Z. et al. The spatial transcriptomic landscape of human gingiva in health and periodontitis. *Sci China Life Sci.* <https://doi.org/10.1007/s11427-023-2467-1> (2023).
32. Zhang, B. et al. Single-cell transcriptional profiling reveals immunomodulatory properties of stromal and epithelial cells in periodontal immune milieu with diabetes in rats. *Int. Immunopharmacol.* **123**, 110715. <https://doi.org/10.1016/j.intimp.110715> (2023).
33. Zong, Y. et al. Ginsenoside Rg1 improves inflammation and autophagy of the pancreas and spleen in Streptozotocin-Induced type 1 diabetic mice. *Int. J. Endocrinol.* **2023**, 3595992. <https://doi.org/10.1155/2023/3595992> (2023).
34. Wang, Z. et al. Ginsenoside Rg1 prevents bone marrow mesenchymal stem cell senescence via NRF2 and PI3K/Akt signaling. *Free Radic Biol. Med.* **174**, 182–194. <https://doi.org/10.1016/j.freeradbiomed.2021.08.007> (2021).
35. Li, S., Yang, W., Li, A., Zhang, L. & Guo, L. Protective effect of Nrf2 in periodontitis - A preclinical systematic review and meta-analysis. *Arch Oral Biol* **151**, 105713. <https://doi.org/10.1016/j.archoralbio.105713> (2023).
36. Bagger, F. O. et al. BloodSpot: a database of gene expression profiles and transcriptional programs for healthy and malignant haematopoiesis. *Nucleic Acids Res* **44**, D917–D924. <https://doi.org/10.1093/nar/gkv1101> (2016).
37. Suzuki, T. et al. Systemic activation of NRF2 alleviates lethal autoimmune inflammation in scurfy mice. *Mol. Cell. Biol.* **37**, e00063–17. <https://doi.org/10.1128/MCB.00063-17> (2017).
38. Xu, Y. et al. Isorhamnetin alleviates airway inflammation by regulating the Nrf2/Keap1 pathway in a mouse model of COPD. *Front. Pharmacol.* **13**, 860362. <https://doi.org/10.3389/fphar.2022.860362> (2022).
39. Dong, J. et al. NRF2 is a critical regulator and therapeutic target of metal implant particle-incurred bone damage. *Biomaterials* **288**, 121742. <https://doi.org/10.1016/j.biomaterials.2022.121742> (2022).
40. Zhang, Z. et al. Maresin1 Suppresses High-Glucose-Induced Ferroptosis in Osteoblasts via NRF2 Activation in Type 2 Diabetic Osteoporosis. *Cells* **11**, 2560. <https://doi.org/10.3390/cells11162560> (2022).
41. Chen, Y. et al. Single-cell RNA landscape of the osteoimmunology microenvironment in periodontitis. *Theranostics* **12**, 1074–1096. <https://doi.org/10.3390/cells11162560> (2022).
42. Gong, W. et al. Orcinol glucoside improves senile osteoporosis through attenuating oxidative stress and autophagy of osteoclast via activating Nrf2/Keap1 and mTOR signaling pathway. *Oxid. Med. Cell. Longev.* **2022** (5410377). <https://doi.org/10.1155/2022/5410377> (2022).
43. Moiseev, D. et al. A new way to model periodontitis in laboratory animals. *Dent. J. (Basel)* **11**, 219. <https://doi.org/10.3390/dj11090219> (2023).
44. He, S. et al. Chloroquine and 3-Methyladenine attenuates periodontal inflammation and bone loss in experimental periodontitis. *Inflammation* **43**, 220–230. <https://doi.org/10.1007/s10753-019-01111-0> (2020).
45. Woitowich, N. C., Beery, A. & Woodruff, T. A 10-year follow-up study of sex inclusion in the biological sciences. *Elife* **9**, e56344. <https://doi.org/10.7554/eLife.56344> (2020).

Author contributions

Yang Zhou and Yunan Zhang : Methodology, Validation, Formal analysis, Investigation, Writing–Original draft. Wang Li, Youbo Liu and Zhongke Wang : Formal analysis, Investigation, Writing–review & editing. Ling Guo : Conceptualization, Supervision, Funding acquisition, Writing– review & editing. All authors have read and agreed to the published version of the manuscript.

Funding

This research was funded by Luzhou Science and Technology Bureau [Grant number 2022-GYF-11].

Declarations

Competing interests

The authors declare no competing interests.

Additional information

Supplementary Information The online version contains supplementary material available at <https://doi.org/10.1038/s41598-025-92165-8>.

Correspondence and requests for materials should be addressed to L.G.

Reprints and permissions information is available at www.nature.com/reprints.

Publisher's note Springer Nature remains neutral with regard to jurisdictional claims in published maps and institutional affiliations.

Open Access This article is licensed under a Creative Commons Attribution-NonCommercial-NoDerivatives 4.0 International License, which permits any non-commercial use, sharing, distribution and reproduction in any medium or format, as long as you give appropriate credit to the original author(s) and the source, provide a link to the Creative Commons licence, and indicate if you modified the licensed material. You do not have permission under this licence to share adapted material derived from this article or parts of it. The images or other third party material in this article are included in the article's Creative Commons licence, unless indicated otherwise in a credit line to the material. If material is not included in the article's Creative Commons licence and your intended use is not permitted by statutory regulation or exceeds the permitted use, you will need to obtain permission directly from the copyright holder. To view a copy of this licence, visit <http://creativecommons.org/licenses/by-nc-nd/4.0/>.

© The Author(s) 2025